Journal of Basic and Applied Engineering Research
p-ISSN: 2350-0077; e-ISSN: 2350-0255; Volume 3, Issue 9; April-June, 2016, pp. 740-745

http://www.krishisanskriti.org/Publication.html

Bio-magnetic Convection in a Pulsatile Rheological Fluid Flow in Channel Filled with Saturated Porous Medium

S. Rawat[1], R. Bansal[2] and S. Kapoor[3]

[1](Mathematics Group), Department of General Studies,Jubail University College (Male Branch), Jubail Industrial City 31961, Kingdom of Saudi Arabia,
[2]Department of Mathematics, IFTM University Moradabad, & PGT (Maths), C.L. Gupta World School, Moradabad
[3]Mathematics, Department of Education in Science and Mathematics, Regional Institute of Education(NCERT), Bhubneshwar , India,
E-mail: [1]sam.rawat@gmail.com, [2]rg12794@gmail.com, [3]saurabh09.iitr@gmail.com

Abstract—*The present paper reports the Bio-Magnetic convection in a pulsatile rheological fluid flow in a channel filled with porous medium. The heat transfer in a non-Newtonian biofluid through a saturated non-Darcian porous medium channel is also discussed. Here the lower and upper plate are at different temperature. The upper is heated whereas the lower one is cooled. The Nakamura-Sawada rheological model is adopted during the study due to higher yield stress than the Casson model. The Forchheimer model is adopted in the momentum equation to simulate blood vessel blockage with deposits in the cardiovascular system. The viscous heating is also introduced in the energy equation. The physical model is formed in the form of the set of coupled PDE. The similarity transformation process is taken into account to transformed the system of PDE into system of nonlinear, coupled ordinary differential equations. The complete system of equation is solved using FEM method. The study of different physical parameter is presented graphically. Spatial-temporal velocity and temperature profile visualizations are also presented. Numerical results shows that normalized fluid velocity (U) increases throughout the channel (-1 < Y < 1) with an increase in Reynolds number, Darcian parameter, steady pressure gradient parameter and rheological parameter; conversely velocity is decreased with increasing magnetic parameter and Forchheimer quadratic drag parameter*

Keywords*: Bio-Magnetic convection; porous media; rheology; heat transfer; pulsatile; numerical, FEM Method.*

1. INTRODUCTION

These The study of pulsating flows is of practical engineering importance. High speed (turbulent) pulsating flows occur in turbo machinery, rotor blade aerodynamics, reciprocating piston-driven flows, etc. Numerous experimental investigations were focused on fundamental studies of fully developed periodic pipe flows with sinusoidal varying pressure gradients (or flow rates). Low speed (laminar) pulsating flows were studied in order to analyze the flows through small pipes or in the blood circulation systems. Laminar flows are relatively simple for analytical (or numerical) analysis and are a natural choice to provide basic studies of fundamental hydrodynamic effects in pulsating flows [1]. Pulsatile flow has also recently found renewed significance in its application to MEMS microfluidic engineering applications [2]. A complete treatment of the fluid dynamics of steady and pulsatory flow with emphasis on basic mechanics, physics and applications can be seen in [3].

Many researchers has contributed in this area. Sharma and Kapoor [4] presented a finite element solution of the Navier-Stokes equations for steady flow under a magnetic field via a double-branched two-dimensional section of a three-dimensional model of the canine aorta in a curvilinear boundary-fitted co-ordinate system.

A finite element technique is used by Bhargava et al. [5] to analyze pulsating magnetohydrodynamic blood flow and species diffusion in a porous medium channel using the Darcy-Forchheimer model. The Newtonian biomagnetic flow of blood in a Darcy-Forchheimer porous regime was studied by Bég et al [6].

Very recently Sharma et al[7] study a mathematical model for the hydro-magnetic non-Newtonian blood flow in the non-Darcy porous medium with a heat source and Joule effect is proposed. they finds its applications in surgical operations, industrial material processing and various heat transfer operations.

Hayat et al. [8] have studied the influence of heat transfer in an MHD second grade fluid film over an unsteady stretching sheet. Vasudev et al. [9] have investigated the influence of magnetic field and heat transfer on peristaltic flow of Jeffrey fluid through a porous medium in an asymmetric channel. They studied the effects of magnetic field and heat transfer on

oscillatory flow of Jeffrey fluid through a porous medium in a circular tube.

More recently [11-17] studied have been made in this mathematical modeling. In the present problem we study the pulsatile magneto-rheological blood flow and heat transfer under transverse magnetic field with viscous heating effects through a Darcy-Forchheimer porous medium channel cooled at the lower plate and heated at the upper, using the Nakamura-Sawada bi-viscosity non-Newtonian model.

2. MATHEMATICAL FORMULATION

Consider the unsteady, two dimensional, laminar, incompressible, electrically-conducting pulsating, bio-rheological fluid flow between two parallel plates intercalating an isotropic, homogenous, saturated, Darcy-Forchheimer porous medium. The two plates are located at a distance *2H* apart with reference to an (x, y) coordinate system, where x defines the longitudinal coordinate parallel to the plates and y the transverse coordinate, perpendicular to the wall. The lower plate is kept at temperature T_1 and upper plate at temperature T_2 such that $T_1 < T_2$. In the present model, the pulsatory character of the physiological flow is generated by a source at infinity, (the actual pulsatile flow is due to the pumping of the heart in the human cardiovascular system). The physical model is shown in fig. 1. In order to simulate the inertial drag effects imparted by the porous matrix in higher velocity flow, the Darcy-Forchheimer model is used. Magnetic Reynolds number is assumed to be small enough to neglect induced magnetic field effects and the applied magnetic field is uniform. The absence of an electrical field also allows exclusion of the effect of polarization of the ionized biofluid (blood). Joule heating effects are also ignored.

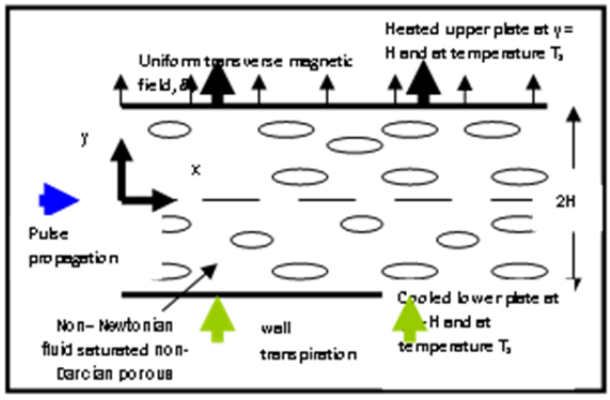

Fig. 1: Physical Model and Coordinate System

Wall transpiration is present at both plates via injection at the lower plate (y = -H) and suction at the upper plate (y = +H). A stress tensor τ_{ij} is introduced into the momentum equation to take into account the rheological characteristic of the blood. We employ the bi-viscosity rheological model which is defined as follows:

$$\tau_{IJ} = \begin{Bmatrix} 2\left[\mu_B + \frac{P_y}{\sqrt{2\pi}}\right] e_{ij}, \pi > \pi_C \\ 2\left[\mu_B + \frac{P_y}{\sqrt{2\pi_C}}\right] e_{ij}, \pi < \pi_C \end{Bmatrix} (1)$$

where $\pi = e_{ij}e_{ij}$ and e_{ij} is the $(i,j)^{th}$ component of the deformation rate, π_c is a critical value of this product based on the Nakamura-Sawada model, μ_B is plastic dynamic viscosity of the non-Newtonian fluid and P_y is yield stress of the fluid. Since the channel walls are infinitely long, the flow variables (velocity, temperature) are purely functions of y and τ. The system of equations governing the flow and energy is therefore given by:

Linear Momentum Equation:

$$\frac{\partial u}{\partial \tau} + V_0 \frac{\partial u}{\partial y} + \frac{1}{\rho}\frac{\partial P}{\partial x} = v_B\left(1 + \frac{1}{\beta}\right)\frac{\partial^2 u}{\partial y^2} - \frac{\sigma B_0^2}{\rho}u - \frac{v_B}{k_p}u - bu^2 \quad (2)$$

Energy (Heat) Equation:

$$\frac{\partial T}{\partial \tau} + V_0 \frac{\partial T}{\partial y} = \alpha \frac{\partial^2 T}{\partial y^2} + \frac{v_B}{k_p c_p}u^2 + \frac{b}{c_p}u^3 \quad (3)$$

The corresponding boundary conditions on the horizontal plate surfaces are:

$y = -H: u = 0, T = T_1$ (4a)

$y = H: u = 0, T = T_2$ (4b)

where μ is Newtonian dynamic viscosity, V_0 is wall transpiration velocity ($V = V_0$) at the lower plate and $V = -V_0$ at the upper plate), β denotes the upper limit of the apparent viscosity coefficient, where u is the x-direction (longitudinal velocity), P is the hydrodynamic pressure, μ is the dynamic viscosity, k_p is hydraulic conductivity (permeability) of the porous material, ρ is the density of the fluid, b is a Forchheimer (inertial drag) coefficient related to the porous medium geometry, τ is the dimensional time, σ is the electrical conductivity of the biofluid (assumed constant), B_o is the transverse magnetic field strength, α is thermal diffusivity, c_p is the specific heat capacity of the biofluid, T denotes biofluid temperature and ∂P/∂x denotes longitudinal pressure gradient. Proceeding with the analysis we now normalize the flow model using the following transformations:

$$U = \frac{u}{V_0}, X = \frac{x}{H}, Y = \frac{y}{H}, t = \frac{V_0}{H}\tau, P^* = \frac{P}{\rho V_0^2}$$

$$\theta = \frac{T - T_m}{T_2 - T_m}, Pr = \frac{v_B}{\alpha}, Re = \frac{HV_0}{v_B}, Nm = \frac{\sigma B_0^2 H}{\rho V_0}, \lambda = \frac{k_p V_0}{v_B H}, N_F = Hb, Ec = \frac{V_0^2}{c_p(T_2 - T_m)},$$

where X and Y are dimensionless coordinates parallel and transverse to the channel walls respectively, U is the transformed velocity component in the X-direction, P* is the

transformed hydrodynamic pressure (* dropped for convenience in analysis), t is dimensionless time, θ is dimensionless temperature, Re is a transpiration Reynolds number, Nm is the hydromagnetic parameter, λ is a Darcian (permeability) parameter, N_F is the Forchheimer (quadratic porous drag) parameter, $T_m = \frac{T_1+T_2}{2}$ is the characteristic temperature, Pr is the Prandtl number and Ec is the Eckert Number. Introducing (5) into equations (1)-(3) leads to the following set of non-linear, coupled, ordinary differential equations:

Momentum Equation:

$$\frac{\partial U}{\partial t} + \frac{\partial U}{\partial Y} = \frac{\partial P}{\partial x} + \frac{1}{Re}\left[1 + \frac{1}{\beta}\right]\frac{\partial^2 U}{\partial Y^2} - NmU - \frac{1}{\lambda}U - N_F U^2 \quad (6)$$

Energy Equation:

$$\frac{\partial \theta}{\partial t} + \frac{\partial \theta}{\partial Y} = \frac{1}{PrRe}\frac{\partial^2 \theta}{\partial Y^2} + \frac{Ec}{\lambda}U^2 + N_F Ec U^3 \quad (7)$$

The transformed spatial boundary conditions now become:

$$At\ Y = -1 : U = 0, \theta = -1 \quad (8a)$$

$$At\ Y = -1 : U = 0, \theta = 1 \quad (8b)$$

Similar thermal boundary conditions (i.e. negative at one wall and positive at the other) were employed recently by Grosan and Pop (2007) in their study of fully-developed mixed radiative-convection in a vertical channel. The pressure gradient is decomposed into a steady component and an imposed (oscillatory) component as follows:

$$-\frac{\partial P}{\partial X} = \left(\frac{\partial P}{\partial X}\right)_s + \left(\frac{\partial P}{\partial X}\right)_o e^{i\omega t} \quad (9)$$

where $(\ )_s$ is the steady component and $(\ )_o$ is oscillating component. This approach had already been implemented extensively in pulsatile flow studies.

3. NUMERICAL SOLUTION BY THE FINITE ELEMENT METHOD

The transformed two-point boundary value problem defined by equations (6,7) with boundary and initial conditions (8a,b) has been solved using the finite element method (FEM). FEM has been shown to be highly versatile and extremely accurate in fluid dynamics analysis. To solve the current coupled, nonlinear problem, we first redefine the pressure gradient as:

$$-\frac{\partial P^*}{\partial X} = P_s + P_o(\cos w^* t) \quad (10)$$

Using equation (10) the momentum equation (6) now becomes:

$$\frac{\partial U}{\partial t} + \frac{\partial U}{\partial Y} = P_s + P_o(\cos w^* t) + \frac{1}{Re}\left[1 + \frac{1}{\beta}\right]\frac{\partial^2 U}{\partial Y^2} - NmU - \frac{1}{\lambda}U - N_F U^2 \quad (11)$$

The initial *temporal* condition is defined as:

$$At\ t = 0 : U = 0, \theta = -1 \quad (12)$$

The whole domain is divided into a set of 82 *line elements* of equal width, each element being two-noded. A number of stages are inherent in the analysis. We consider these in turn now.

Variational Formulation:

The variational form associated with equations (14), (7) over a typical two-noded linear element (Y_e, Y_{e+1}) is given by:

$$\int_{Y_e}^{Y_{e+1}} w_1 \left\{\frac{1}{Re}\left[1 + \frac{1}{\beta}\right]\frac{\partial^2 U}{\partial Y^2} - \frac{\partial U}{\partial Y} - NmU - \frac{1}{\lambda}U - N_F U^2 - \frac{\partial U}{\partial t} + P_s + P_o(\cos w^* t)\right\} dY = 0 \quad (13)$$

$$\int_{Y_e}^{Y_{e+1}} w_2 \left\{\frac{1}{PrRe}\frac{\partial^2 \theta}{\partial Y^2} + \frac{Ec}{\lambda}U^2 + N_F Ec U^3 - \frac{\partial \theta}{\partial Y} - \frac{\partial \theta}{\partial t}\right\} dY = 0 \quad (14)$$

where w_1 and w_2 are arbitrary test functions and may be viewed as the variation in U and θ respectively.

Finite Element Formulation:

The finite element model may be obtained from equations (16)-(17) by substituting finite element approximations of the form:

$$U = \sum_{j=1}^{2} U_j \psi_j, \theta = \sum_{j=1}^{2} \theta_j \psi_j \quad (15)$$

With $w_1 = w_2 = \psi_i\ (i = 1,2)\ where\ \psi_i$ are the shape functions for a typical element(Y_e, Y_{e+1}) and are defined thus:

$$\psi_1^{(e)} = \frac{Y_{e+1} - Y}{Y_{e+1} - Y_e}, \psi_2^{(e)} = \frac{Y - Y_e}{Y_{e+1} - Y_e}\ Y_e \le Y \le Y_{e+1} \quad (16)$$

The finite element model of the equations for a typical element(Y_e, Y_{e+1}) thus formed is given by:

$$\begin{bmatrix}[K^{11}] & [K^{12}] \\ [K^{21}] & [K^{22}]\end{bmatrix}\begin{bmatrix}\{U\} \\ \{\theta\}\end{bmatrix} + \begin{bmatrix}[M^{11}] & [M^{12}] \\ [M^{21}] & [M^{22}]\end{bmatrix}\begin{bmatrix}\{U\} \\ \{\theta\}\end{bmatrix} = \begin{bmatrix}\{F^1\} \\ \{F^2\}\end{bmatrix} \quad (17)$$

where $[K^{mn}]$, $[M^{mn}]$, and $[F^m]$, (m ,n=1,2) are matrices of order 2x2, 2x2, and 2x1, respectively. Also U_i and θ_i are derivatives of U_i and θ_i with respect to t. All these matrices may be defined as follows:

$$K_{ij}^{11} = -\frac{1}{Re}\left[1 + \left(\frac{1}{\beta}\right)\right]\int_{Y_e}^{Y_{e+1}} \frac{d\psi_i}{dY}\frac{d\psi_j}{dY} dY - \int_{Y_e}^{Y_{e+1}} \psi_i \frac{d\psi_j}{dY} dY - Nm\int_{Y_e}^{Y_{e+1}} \psi_i \psi_j dY - \frac{1}{\lambda}\int_{Y_e}^{Y_{e+1}} \psi_i \psi_j dY - N_F \overline{U_1}\int_{Y_e}^{Y_{e+1}} \psi_i \psi_1 \psi_k dY - N_F \overline{U_1}\int_{Y_e}^{Y_{e+1}} \psi_i \psi_2 \psi_k dY$$

$$K_{ij}^{12} = 0,$$

$$K_{ij}^{21} = \psi_i \psi_1 \psi_j dY + Yfdkj \quad \frac{E_c}{\lambda}\overline{U_1}\int_{Y_e}^{Y_{e+1}} \quad N_F E_c \overline{U_2}^2 \int_{Y_e}^{Y_{e+1}} \psi_i \psi_2^2 \psi_j dY \cdot \quad \frac{E_c}{\lambda}\overline{U_2}\int_{Y_e}^{Y_{e+1}} \psi_i \psi_2 \psi_j dY + N_F E_c \overline{U_1}^2 \int_{Y_e}^{Y_{e+1}} \psi_i \psi_1^2 \psi_j dY + N_F E_c \overline{U_1}\overline{U_2}\int_{Y_e}^{Y_{e+1}} \psi_i \psi_1 \psi_2 \psi_j dY \P$$

$$K_{ij}^{22} = -\frac{1}{PrRe}\int_{Y_e}^{Y_{e+1}} \frac{d\psi_i}{dY}\frac{d\psi_j}{dY} dY - bjbkj \int_{Y_e}^{Y_{e+1}} \psi_i \frac{d\psi_j}{dY} dY$$

$$M_{ij}^{11} = -\int_{Y_e}^{Y_{e+1}} \psi_i \psi_j dY, M_{ij}^{12} = M_{ij}^{21} = 0, M_{ij}^{22} = -\int_{Y_e}^{Y_{e+1}} \psi_i \psi_j dY,$$

(18)

$$M_{ij}^{11} = -\int_{Y_e}^{Y_{e+1}} \psi_i \psi_j dY,$$

$M_{ij}^{12} = M_{ij}^{21} = 0$, $M_{ij}^{22} = -\int_{Y_e}^{Y_{e+1}} \psi_i \psi_j dY$ (19)

$F_i^1 = -\frac{1}{Re}\left[1 + \left(\frac{1}{\beta}\right)\right]\left(\psi_i \frac{d\psi_j}{dY}\right)_{Y_e}^{Y_{e+1}} - \int_Y^{Y+} \psi_i (P_s +$
$P_o(\cos w^* t)\, dY$ (20)

$$F_i^2 = -\frac{1}{PrRe}\left(\psi_i \frac{d\theta}{dY}\right)_{Y_e}^{Y_{e+1}} \quad (21)$$

where $\bar{U} = \sum_{i=1}^{2} \bar{U}_i \psi_i$ and each element matrix is of the order 4×4. Following assembly of all the element equations we obtain a matrix of order 166 x 166. This system of equations is non-linear and is linearized by incorporating the functions $\bar{U}$ which are assumed to be known. After applying the given boundary conditions only a system of 162 equations remain then to be solved and this is performed iteratively by the Gauss-Seidel method maintaining an accuracy of 0.0005.

4. GRAPHICAL RESULTS AND DISCUSSION

Numerical simulations have been performed to study the effect of Reynolds number (Re), rheological parameter (β), steady component of pressure gradient (Ps), Darcy number (λ), Forchheimer number (N_F), hydromagnetic parameter (Nm), Eckert number (Ec) and Prandtl number (Pr) on velocity, *U,* and temperature, θ profiles across the channel (Y) with time, *t*. We assume blood (ρ = 1050 kg m^{-3}) flows between plates located at distance 2H = 1 × 10^{-2}m with suction V_o = 0.01 × 10^{-2} ms^{-1} to obtain physically realistic computations . For this data, transpiration Reynolds number Re is equal to 0.2(approx.). The Prandtl number (Pr) can be considered constant since the viscosity μ and specific heat under constant pressure c_p and the thermal conductivity (k) of any fluid, and of the blood are temperature-dependent.

Characteristic values of μ, c_p, k are taken as 3.2 ×1 0^{-3} $Kgm^{-1}s^{-1}$, 14.65 J Kg^{-1} K^{-1} and 2.2 × 10^{-3} J m^{-1} s^{-1} K^{-1} respectively. Following this data we also specify Pr = 21 and Ec = 6.2 × 10^{-11} as default values in the computations. The Eckert number signifies the amount of mechanical energy dissipated as thermal energy in the flow. The electrical conductivity (σ) of stationary blood has been quantified as 0.7 s m^{-1} . Since the electrical conductivity of flowing blood is always greater than that of stationary blood, in the present study we elect to use a slightly higher value of 0.8 s m^{-1} and conductivity is assumed to be temperature-independent for simplicity. According to our computations the default values of the control parameters are: Reynolds number (Re) = 0.2, non-Newtonian parameter (β) = 4, dimensionless angular frequency (ω*) = 8, steady component of presure gradient (Ps) = 8, pulsating amplitude (Po) = 5, Darcian parameter (λ) = 0.7, Forchheimer parameter (N_F) = 0.03 (which corresponds to very weak inertial effects), magnetic field (Nm) = 2.4, Eckert number (Ec) = 6.2 × 10^{-11} and Prandtl number (Pr) = 21, unless otherwise stated.

In order to obtain the accuracy of our results, comparisons have been made with the finite difference method . Excellent correlation can be observed between both methods for the dimensionless velocity profile (U) with transverse coordinate (Y). Spatial-temporal variations of the velocity and temperature fields for various flow cases are shown in figures 2 a ,b, Fig. 3 and Fig. 4. **Figs. 2(a) and 2(b)** shows the velocity, *U* and temperature, θ, profiles with respect to both space Y and time t for the general flow case. In Fig. 2a the oscillatory nature of the flow is clear with *peak velocities always corresponding to the centre of the channel*. With increase in time, the magnitude of these peaks is increased. On the other hand in Fig. 2b the temperature (θ) distribution is *not oscillatory* in nature and descends smoothly for all time, from a maximum of 1 at the upper plate (Y = 1) to -1 at the lower plate (Y = -1).

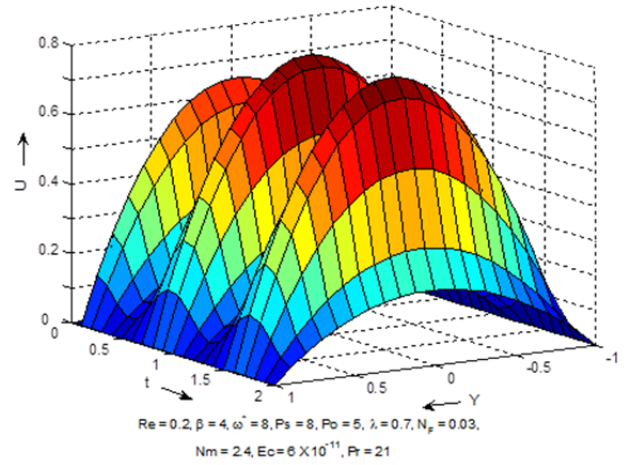

Fig. 2a: Non- Dimensional velocity profile (U) versus transverse coordinate (Y) and time (t) for the general magneto-bio-rheological, non-Darcian case.

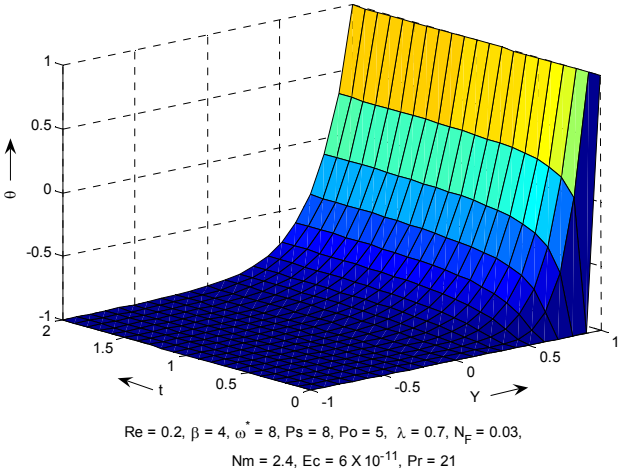

Fig. 2b: Non-Dimensional temperature profile (θ) versus transverse coordinate (Y) and time (t) for the general magneto-bio-rheological, non-Darcian case.

In **figs. 3 to 7**, presented the *spatial* distributions of temperature and velocity , each at t = 0.5, for variation of different control parameters in the model.

Fig. 3 shows the influence of the transpiration Reynolds number on velocity profile at time t = 0.5. As expected, an increase in Reynolds number from 0.05 to 1 increases the fluid velocity i.e. accelerates flow across the channel. The profiles although generally parabolic are increasingly skewed to the right i.e. towards the upper plate (Y = 1), with an increase in Re since this parameter incorporates the suction velocity (V_o) i.e. with greater Re values suction at the upper plate will be enhanced which will serve to displaces the velocity distribution towards the upper plate.

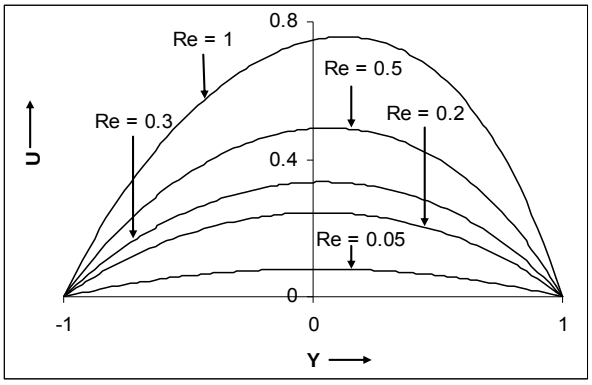

Fig. 3: U versus Y for various transpiration Reynolds numbers (Re) at t = 0.5

Fig. 4 shows the influence of rheological parameter, β, on fluid velocity at time t = 0.5. Smaller value of this parameter correspond to *stronger non-Newtonian behaviour* (i.e. a rise in the viscosity) which will decelerate the flow and reduce longitudinal fluid velocity, U. $\beta \to \infty$ represents the case of a Newtonian fluid which corresponds to the *lowest* value of fluid viscosity and contributes to the *maximum* velocity computed. β =1 corresponds to strongly rheological flow at higher viscosity and results in the minimization of fluid velocity, U across the channel.

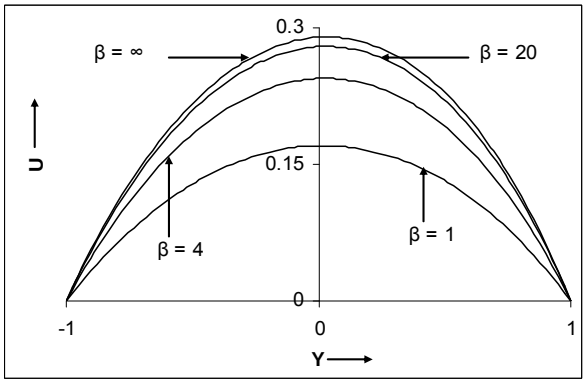

Fig. 4: U versus Y for various non-Newtonian parameter values (β) at t = 0.5

Fig. 5 depicts the effect of hydromagnetic parameter, *Nm*, on velocity profile at time t = 0.5. Decrease in the velocity of bio-rheological fluid due to the increase in the retarding force (Lorentz body force) generated by the magnetic field as Nm increses.

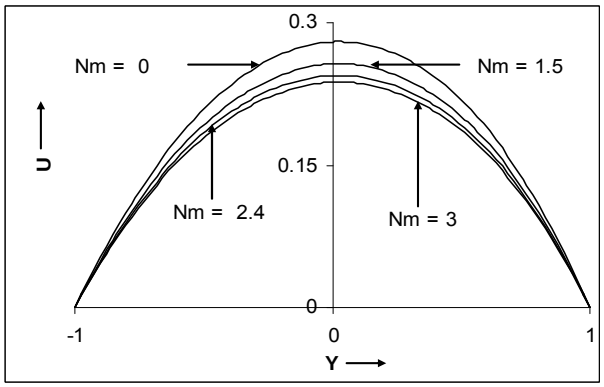

Fig. 5: U versus Y for various hydromagnetic parameter values (Nm) at t = 0.5

Fig. 6 shows the influence of Eckert Number Ec on temperature profile at time t = 0.5. Ec quantifies the ratio of kinetic energy of the flow to the enthalpy difference. Very small mechanical energy is dissipated as heat in the fluid i.e. no warming effect occurs throughout the entire lower semi-section of the channel (-1<Y<0) where temperatures remain negative when Ec value is low i.e. 6.2×10^{-11}. The negativity of temperature is forced by the lower boundary condition (θ = -1 at Y = -1 in 8a). This negative temperature behaviour is sustained throughout most of the upper semi-section of the channel also (0< Y < 0.9) until temperatures cross-over very close to the upper heated plate at Y ~ 0.9. We observe that there is a considerable increase in the temperature profiles for higher Ec value (Ec=3)as depicted by Fig.6 . This effect is clearly absent at the very low values of Ec since the viscous heating term has negligible effect at these values.

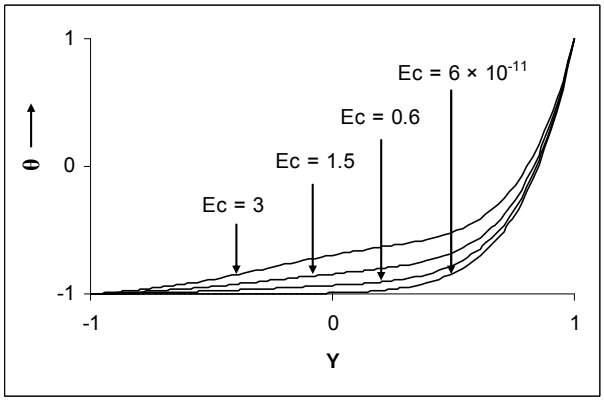

Fig. 6: θ versus Y for various Eckert numbers (Ec) at t = 0.5

Finally in **Fig. 7** depicts the effect of Prandtl number on temperature profiles (θ) . Pr is the ratio of momentum diffusivity to thermal diffusivity. Larger Pr fluids (Pr >1) will diffuse momentum faster than heat. For Pr = 1 the momentum and energy will be diffused at the same rate. Increasing Pr from 1 through 5, 10 and 21 therefore will *decrease* temperatures of the biofluid in the channel, as observed in Fig. 7. In consistency with the spatial boundary conditions temperatures increases from the minimum value of -1 at the lower plate to the maximum value of 1 at the upper plate.

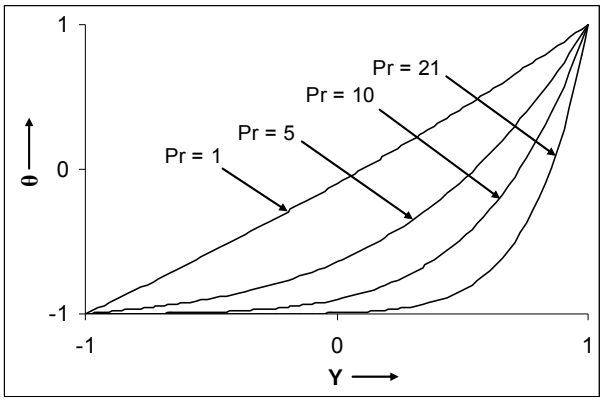

Fig. 7: θ versus Y for various Prandtl numbers (Pr) at t = 0.5

5. CONCLUSIONS

In the present study, the pulsatile Bio-magneto-rheological blood flow through a horizontal channel containing a porous medium in the presence of a transverse magnetic field with viscous heating performed numerically using the FEM. Numerical results have shown that an increase in Darcy parameter (λ), transpiration Reynolds number (Re), rheological parameter (β) , Prandtl number (Pr) and Ecret number (EC) here the steady shows the component of pressure gradient (Ps) accelerates the fluid flow, whereas fluid velocity is reduced with an increase hydromagnetic number. A major increase is observed in temperature profile for high Eckert numbers, which is absent when Ec is small. The results indicate that the magnetic field has a considerable effect on the velocity profile as does the porous medium and the biofluid rheology. There is some other instersting results depicted in other physical parameter.

REFERENCES

[1] Yakhot, M. Arad, G. Ben-Dor, Numerical investigation of a laminar pulsating flow in a rectangular duct, Int. J. Numer. Meth. Fluids 29, (1999), 935-950

[2] F. Fedele, D. Hitt, R. D. Prabhu, Revisiting the stability of pulsatile pipe flow, Eur. J. Mech., B, Fluids, 24 (2005), 237–254.

[3] M. Zamir, The Physics of Pulsatile Flow, Springer-Verlag, New York, 2000

[4] Sharma, G.C. and Kapoor, J.C., Finite element computations of two-dimensional arterial flow in the presence of a transverse magnetic field, Int. J. Numerical Methods Fluids, **20, 10**,**1153 - 1161 (1995).**

[5] Bhargava, R., S. Rawat, H.S. Takhar, Bég, O.A., Pulsatile magneto-biofluid flow and mass transfer in a non-Darcian porous medium channel, Meccanica, 42, 247–262, 2007.

[6] Bég, O.A., T. A. Bég, R. Bharagava, Rawat, S., H. S. Takhar, T-K Hung, Numerical analysis of biomagnetic Newtonian flow in a Darcy-Forchheimer porous medium, J. Theoretical and Applied Mechanics, 32, 3, 20-45 (2007).

[7] Sharma, B. K., et al. "Mathematical Modeling of Magneto Pulsatile Blood Flow Through a Porous Medium with a Heat Source." International Journal of Applied Mechanics and Engineering 20.2 (2015): 385-396.

[8] T. Hayat, S. Saif and Z. Abbas, The influence of heat transfer in an MHD second grade fluid film over an unsteady stretching sheet, Physics Letters A ,372 (2008), 5037-5045.

[9] C. Vasudev, U. Rajeswara Rao, M. V. Subba Reddy and G. Prabhakara Rao, Influence of magnetic field and heat transfer on peristaltic flow of Jeffrey fluid through a porous medium in an asymmetric channel, ARPN Journal of Engineering and Applied Sciences, 5(12)(2010), 87-103.

[10] K. Srinivasa Rao & P. Koteswara Rao,"Effect Of Heat Transfer On Mhd oscillatory flow of jeffrey fluid through a porous medium in a tube "international journal of mathematical archive-3(11), 2012, 4692-4699

[11] S Rawat, R Bhagrava, S Kapoor, O Anwar Beg ," Heat and mass Transfer of a Chemically Reacting Micropolar Fluid Over a Linear Streaching Sheet in Darcy Forchheimer Porous Medium ",International Journal of Computer Applications 44 (6), (2012) , 40-51

[12] S Kapoor, P Alam, R Gupta, LM Tiwari, S Aggarwal, "Analytical study of MHD natural convective flow of incompressible fluid flow from a vertical flat plate in porous medium ",Modeling, Simulation and Applied Optimization (ICMSAO), 2011 , IEEE Xplore, pp, 1-6

[13] S Rawat, R Bhargava, S Kapoor, OA Bég, TA Bég, R Bansal ," Numerical Modeling of Two-Phase Hydromagnetic Flow and Heat Transfer in a Particle-Suspension through a non-Darcian Porous Channel.", Journal of Applied Fluid Mechanics 7 (2), (2014), 249-261

[14] S Kapoor, P Bera, A Kumar ," Effect of Rayleigh Thermal Number in Double Diffusive Non-Darcy Mixed Convective Flow in Vertical Pipe Filled with Porous Medium", Procedia Engineering 38 (2012), 314-320

[15] S Rawat, S Kapoor, R Bhargava ,"MHD Flow Heat and Mass Transfer of Micropolar Fluid over a Nonlinear Stretching Sheet with Variable Micro Inertia Density, Heat Flux and Chemical Reaction in a Non-darcy Porous Medium",Journal of Applied Fluid Mechanics 9 (1), (2016) 321-331

[16] S Rawat, S Kapoor," Finite Element Study of Radiative Free Convection Flow Over a Linearly Moving Permeable Vertical Surface in the Presence of Magnetic Field",Procedia Engineering 38 (2012), 2288-2296

[17] S. Rawat, R .Bhargava, S. Kapoor ," Sensitivity analysis of pulsatile hydromagnetic biofluid flow and heat transfer with non linear Darcy-Forchheimer drag ", Accepted for publication in Journal of Applied Fluid Mechanics 9 (4), (2016) October 2016.